



Cite this: *Dalton Trans.*, 2018, **47**, 16938

## Full compositional control of $\text{PbS}_x\text{Se}_{1-x}$ thin films by the use of acylchalcogourato lead(II) complexes as precursors for AACVD†

Tagbo Emmanuel Ezenwa,<sup>a</sup> Paul D. McNaughten,<sup>id</sup> <sup>\*a</sup> James Raftery,<sup>a</sup> David J. Lewis<sup>id</sup> <sup>a</sup> and Paul O'Brien<sup>id</sup> <sup>\*a,b</sup>

Selenium and sulfur derivatives of lead(II) acylchalcogourato complexes have been used to deposit  $\text{PbS}_x\text{Se}_{1-x}$  thin films by AACVD. By variation of the mole ratio of sulfur and selenium precursors in the aerosol feed solution the full range of compositions of  $\text{PbS}_x\text{Se}_{1-x}$  was obtained, *i.e.*  $0 \leq x \leq 1$ . The films showed no contaminant phases demonstrating the potential for acylchalcogourato metal complexes as precursors for metal chalcogenide thin films. The crystal structure for bis[*N,N*-diethyl-*N'*-2-naphthoylthioureato]lead(II) was solved and displayed the expected decreases in Pb–E bond lengths from the previously reported selenium variant.

Received 23rd August 2018,  
Accepted 26th September 2018

DOI: 10.1039/c8dt03443e

rsc.li/dalton

## Introduction

Lead chalcogenide nanomaterials have potential within photo-voltaic devices due to their advantageous bulk bandgaps in the infra-red region ( $\text{PbS} = 0.41$  eV,  $\text{PbSe} = 0.28$  eV and  $\text{PbTe} = 0.31$  eV) and the ability to tune the band gap by quantum confinement. The production of alloyed lead chalcogenide thin films allows for additional band gap tuning thus giving further control over the region of the electromagnetic spectrum collected. In this work we present a route to  $\text{PbS}_x\text{Se}_{1-x}$  thin films, where  $0 \leq x \leq 1$ , using acylchalcogourea lead(II) complexes as precursors *via* aerosol assisted chemical vapour deposition (AACVD).

AACVD is a well-established technique for the production of thin films of metal chalcogenides. Single source precursors have been used as precursors for thin films by AACVD, which is a well-established route to synthesize a wide range of metal chalcogenides, CdE, PbE, NiE, SnS, ZnE *etc.* and has been reviewed previously by O'Brien *et al.*<sup>1–3</sup> In particular lead chalcogenide films have been produced using lead complexed to dithiocarbamates,<sup>4–6</sup> selenoureas,<sup>7–10</sup> dichalcogenoimido-phosphinates,<sup>5,11–13</sup> dichalcogenophosphates<sup>14,15</sup> and

xanthates<sup>16–21</sup> There are fewer reports on the use of single source precursors forming lead selenides due to the synthesis of noxious carbon diselenide when synthesising dithiocarbamates and xanthates. *N*-Acyl chalcogoureas offer a convenient route to a carbon–chalcogen double bond due to the availability and ease of the use of potassium selenocyanate and potassium thiocyanate as precursors. The ability to use potassium selenocyanate as a precursor for *N*-acylselenoureas is an attractive alternative to common selenium sources, *e.g.* carbon diselenide, as the starting material is potassium selenocyanate, an air stable solid at standard temperature and pressure, and the synthesis of the acylselenourea ligand is performed under air without heating.

Metal *N*-acylchalcogourea complexes have been previously explored to produce binary metal sulfide nanocrystals containing lead or iron by O'Brien *et al.* When using bis[*N,N*-diethyl-*N'*-naphthoylselenoureato]lead(II) in the presence of gold nanoparticles the precursor yielded PbSe nanorods with large aspect ratios, *i.e.* diameters of 8 to 25 nm, and lengths of 100 nm to a micron.<sup>8</sup> By the use of a lower molecular weight complex, bis(*N,N*-diisobutyl-*N'*-(4-nitrobenzoyl)selenoureato)lead(II) Akhtar *et al.* produced PbSe thin films by AACVD and nanocrystals by a solvothermal synthesis.<sup>22</sup> In combination with lead(II) ethylxanthate, bis[*N,N*-diethyl-*N'*-2-naphthoylselenocogoureato]lead(II) was used to produce thin films of  $\text{PbS}_x\text{Se}_{1-x}$  *via* solution processing and thermolysis.<sup>23</sup> The tris(*N,N*-diethyl-*N'*-naphthoylselenoureato)iron(III) analogue was used in AACVD to form FeSe films on silicon substrates and when using solvothermal methods in the presence of oleylamine produced  $\text{FeS}_2$ .<sup>10</sup>

We report the use of the sulfur and selenium derivatives of bis[*N,N*-diethyl-*N'*-2-naphthoylchalcogoureato]lead(II) to syn-

<sup>a</sup>School of Chemistry, The University of Manchester, Oxford Road, Manchester, M13 9PL, UK. E-mail: paul.mcnaughten@manchester.ac.uk, paul.obrien@manchester.ac.uk

<sup>b</sup>School of Materials, The University of Manchester, Oxford Road, Manchester, M13 9PL, UK

† Electronic supplementary information (ESI) available. CCDC 1005699. For ESI and crystallographic data in CIF or other electronic format see DOI: 10.1039/c8dt03443e



thesise  $\text{PbS}_x\text{Se}_{1-x}$  films with controlled compositions of sulfur and selenium. The composition of the films is controlled by variation of the mole fraction of the precursors used in the aerosol feed solution in the AACVD process and shows the expected slight deviation from Vegard's law as expected for  $\text{PbS}_x\text{Se}_{1-x}$ .

## Experimental

### Chemicals used

2-Naphthoyl chloride (98%, Sigma-Aldrich), acetone ( $\geq 99.9\%$ , Sigma-Aldrich), potassium selenocyanate (97%, Sigma-Aldrich), diethylamine ( $\geq 99.5\%$ , Sigma-Aldrich), ethanol ( $\geq 99.8\%$ , Sigma-Aldrich), diethylether ( $\geq 99.8\%$ , Sigma-Aldrich), potassium thiocyanate ( $\geq 99\%$ , Sigma-Aldrich) and tetrahydrofuran ( $\geq 99.9\%$ , Sigma-Aldrich) were used. All syntheses were performed under an inert nitrogen atmosphere and the work ups performed in air.

### Synthesis of *N,N*-diethyl-*N'*-2-naphthoylselenourea (1)

The synthesis of *N,N*-diethyl-*N'*-2-naphthoylselenourea is adapted from the procedure by Douglass *et al.*<sup>24,25</sup> In brief, a solution of 2-naphthoyl chloride (4.61 g, 24.2 mmol) in acetone (30 ml) was added dropwise to a stirred solution of potassium selenocyanate (3.48 g, 24.2 mmol) and was stirred for a further 15 minutes resulting in a green/yellow solution. A solution of diethylamine (1.77 g, 24.2 mmol) in acetone (10 ml) was added dropwise and stirred for 15 minutes resulting in an orange solution. *N,N*-Diethyl-*N'*-2-naphthoylselenourea was extracted from acetone by addition of diethylether (50 ml). The diethylether layer was collected and removed *in vacuo* resulting in a red solid which was recrystallised from warm ethanol to give orange crystals. Yield = 33% elemental analysis: found: C, 55.65; H, 5.60; N, 8.50; calc.: C, 57.66; H, 5.41; N, 8.41.  $^1\text{H}$  NMR (400 MHz,  $\text{CDCl}_3$ )  $\delta$  8.69 (s, 1H, Ar), 8.37 (s, 1H, NH), 7.98–7.84 (m, 4H, Ar), 7.66–7.54 (m, 2H, Ar), 4.18 (q,  $J = 7.1$  Hz, 2H,  $\text{CH}_2$ ), 3.66 (q,  $J = 7.2$  Hz, 2H,  $\text{CH}_2$ ), 1.44 (t,  $J = 7.1$  Hz, 3H,  $\text{CH}_3$ ), 1.35 (t,  $J = 7.2$  Hz, 3H,  $\text{CH}_3$ ).  $^{77}\text{Se}$  NMR (400 MHz,  $\text{CDCl}_3$  with  $\text{PhSeSePh}$ )  $\delta$  479.23 (s, C=Se).  $\nu_{\text{max}}/\text{cm}^{-1}$  1649.1(s) (C=O). M.p. = 134–136 °C.

### Synthesis of *N,N*-diethyl-*N'*-2-naphthoylthiourea (2)

The synthesis of 2 is identical to that of 1 except that potassium thiocyanate (1.96 g, 24.2 mmol) was used in place of potassium selenocyanate and yellow crystals were obtained. Yield = 34% elemental analysis: found: C, 67.26; H, 6.78; N, 9.82; S, 11.08; calc.: C, 67.10; H, 6.30; N, 9.80; S, 11.20.  $^1\text{H}$  NMR (400 MHz,  $\text{CDCl}_3$ )  $\delta$  8.71 (s, 1H, Ar), 8.34 (s, 1H, NH), 8.03–7.74 (m, 4H, Ar), 7.56 (m, 2H, Ar), 4.03 (d,  $J = 6.8$  Hz, 2H,  $\text{CH}_2$ ), 3.63 (d,  $J = 6.9$  Hz, 2H,  $\text{CH}_2$ ), 1.33 (m, 6H,  $\text{CH}_3$ ).  $m/z$  285.0 (M – H 100%)  $\nu_{\text{max}}/\text{cm}^{-1}$  1677.4(s) (C=O). M.p. = 105–106 °C.

### Synthesis of bis[*N,N*-diethyl-*N'*-2-naphthoylselenoureato]lead(II) (3)

The synthesis of bis[*N,N*-diethyl-*N'*-2-naphthoylselenoureato]lead(II) is adapted from the synthesis by Akhtar *et al.*<sup>8</sup> In brief,

2 (2.00 g, 6.0 mmol) was dissolved in 50 ml of warm ethanol followed by the addition of sodium ethoxide (0.41 g, 6.0 mmol). The solution was stirred for 20 minutes and a solution of lead acetate (1.14 g, 3.0 mmol) in ethanol (50 ml) was added dropwise. This was stirred for a further 20 minutes and was allowed to cool to room temperature forming a yellow precipitate. The precipitate was recrystallized from hexane/toluene to give yellow crystals.

Yield = 78% elemental analysis: found: C, 44.30; H, 3.81; N, 6.19; Pb, 23.80; calc.: C, 44.10; H, 3.90; N, 6.19; Pb, 23.68.  $^1\text{H}$  NMR (400 MHz,  $\text{CDCl}_3$ )  $\delta$  8.60 (s, 2H, Ar), 8.12 (dd,  $J = 8.6$ , 1.6 Hz, 2H, Ar), 7.81 (dd,  $J = 31.0$ , 7.8 Hz, 4H, Ar), 7.73 (d,  $J = 8.6$  Hz, 2H, Ar), 7.49–7.34 (m, 4H, Ar), 3.85–3.63 (m, 8H,  $\text{CH}_2$ ), 1.17 (t,  $J = 7.1$  Hz, 6H,  $\text{CH}_3$ ), 1.00 (t,  $J = 7.1$  Hz, 6H,  $\text{CH}_3$ ).  $^{77}\text{Se}$  NMR (400 MHz,  $\text{CDCl}_3$  with  $\text{PhSeSePh}$ )  $\delta$  292.23 (s, C–Se).  $m/z$  873.2 ( $\text{M}^+$ , 100%), 541.1 (78), 111.3 (30), 1409.4 (50). M.p. = 149 °C.

### Synthesis of bis[*N,N*-diethyl-*N'*-2-naphthoylthioureato]lead(II) (4)

The synthesis of 4 is the same as that for 3 except that 2 (1.72 g, 6.0 mmol) was used in place of 1 with colourless crystals being collected following recrystallisation. Yield = 65.3% elemental analysis: found: C, 49.6; H, 4.2; N, 7.2; S, 8.1; Pb, 25.2; calc.: C, 49.4; H, 4.4; N, 7.2; S, 8.2; Pb, 26.7.  $^1\text{H}$  NMR (400 MHz,  $\text{CDCl}_3$ )  $\delta$  8.68 (s, 2H), 8.21 (dd,  $J = 8.6$ , 1.6 Hz, 2H), 7.92–7.77 (m, 6H), 7.49 (m, 4H, Ar), 3.84 (q,  $J = 7.1$  Hz, 4H,  $\text{CH}_2$ ), 3.75 (q,  $J = 7.1$  Hz, 4H,  $\text{CH}_2$ ), 1.23 (t,  $J = 7.1$  Hz, 6H,  $\text{CH}_3$ ), 1.05 (t,  $J = 7.1$  Hz, 6H,  $\text{CH}_3$ ).  $m/z$  779.3 ( $\text{M}^+$ , 100%), 493.1 (38), 287.1 (30), 1270.5 (24). M.p. = 198–199 °C.

### AACVD procedure

In a typical deposition 200 mg of precursor was dissolved in tetrahydrofuran (20 ml). This was placed in a 100 ml round bottom flask with an inlet for the carrier gas (argon) and an outlet connected to an open ended quartz furnace tube. The tube was loaded with eight glass substrates (approx. 1 cm  $\times$  2 cm). The flask and tubing was purged with argon at a flow rate of 200 SCCM for 5 minutes prior to heating to 350 °C using a Carbolite tube furnace. An aerosol was generated by placing the round bottom flask in a water bath above a piezoelectric modulator of a PIFCO ultrasonic humidifier (model 1077) and carried to the furnace tube by the argon flow. Depositions were carried out for 30 minutes at the target temperature before being allowed to cool to room temperature.

### Crystal structure determination

Crystals for single crystal X-ray diffraction studies were grown using vapour diffusion of diethylether into a solution of precursor in chloroform. Measurements were made using graphite monochromated Cu-K $\alpha$  radiation on a Bruker Prospector diffractometer. The structures were solved by direct methods and refined by full-matrix least squares on  $F^2$ . All calculations were carried out using the SHELXTL package Version 6.10.<sup>26</sup> Non-hydrogen atoms were refined with anisotropic atomic displacement parameters. Hydrogen atoms were placed in calculated positions, assigned isotropic thermal parameters and allowed to ride on their parent carbon atoms.



## Instrumentation

Thermogravimetric analysis (TGA) and elemental analysis were performed at the University of Manchester Microanalytical Laboratory, using a Thermo Scientific Flash 2000 organic elemental analyser and a Seiko SSC/S200 under N<sub>2</sub>. TGA profiles were acquired from room temperature to 600 °C with a heating rate of 10 °C min<sup>-1</sup>. Electron microscopy was performed using an FEI XL-30 scanning electron microscope (SEM) in a secondary electron configuration. <sup>1</sup>H NMR spectra were collected using a Bruker AVANCE III 400 MHz spectrometer. X-ray diffraction (XRD) patterns were acquired with a Bruker D8 Advance diffractometer equipped with a Cu K $\alpha$  source.

## Results and discussion

### Precursor characterisation

The structure of bis[*N,N*-diethyl-*N'*-2-naphthoylthioureato]lead(II) is shown in Fig. 1 and Table 1. The structure exhibits a stereo-



Fig. 1 A thermal ellipsoid plot representing the structure of 4. CCDC ref. 1005699.†

Table 1 Selected bond lengths and angles for 4

Bond or angle	Value
Pb(1)–S(1)	2.7080(13) Å
Pb(1)–S(2)	2.6996(12) Å
O(1)–Pb(1)	2.394(3) Å
O(2)–Pb(1)	2.450(3) Å
O(2)–Pb(1)–S(1)	76.09(9)°
S(2)–Pb(1)–S(1)	100.38(4)°

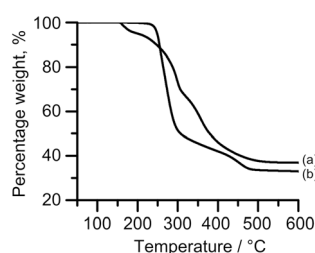


Fig. 2 TGA of 4 & 3 shown as (a) & (b) respectively.

chemically active inert pair resulting in a distorted square pyramidal structure. The structure is similar to that of the previously reported bis[*N,N*-diethyl-*N'*-2-naphthoylselenoureato]

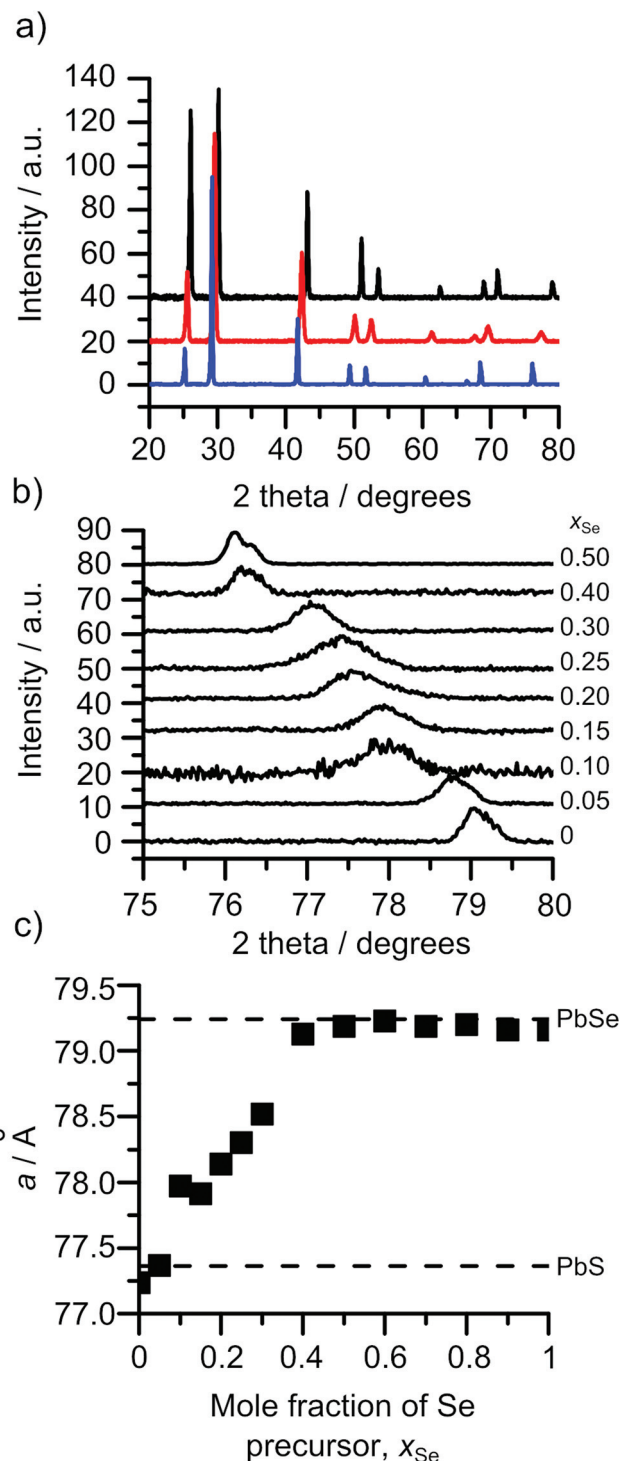


Fig. 3 XRD analysis of the PbS<sub>x</sub>Se<sub>1-x</sub> films. (a) XRD patterns from  $x_{\text{Se}} = 0$  (black),  $x_{\text{Se}} = 0.25$  (red) and  $x_{\text{Se}} = 0.5$  (blue). (b) XRD patterns of the 422 reflection from  $x_{\text{Se}} = 0$  to 0.5. (c) Shows a plot of mole fraction against the position of the 422 reflection as compared to the values from the reference patterns (PbSe ICDD 00-006-0354 and PbS ICDD 00-005-0592) shown with dashed lines.





lead(II) with the exception of the Pb–S bonds being on average 0.8 Å shorter than their Pb–Se equivalents.<sup>8</sup>

The TGA profiles show considerable differences between the breakdown of the sulphur (a) and selenium (b) precursors, Fig. 2. From the first derivatives of the TGA profiles, ESI Fig. 1,<sup>†</sup> it can be seen that bis[*N,N*-diethyl-*N'*-2-naphthoylthioureato]lead(II), (a), has an onset at 146.3 °C and a three step decomposition whereas bis[*N,N*-diethyl-*N'*-2-naphthoylselenoureato]lead(II), (b), has a higher onset temperature at 210.6 °C and a two-step decomposition. This difference in the number of steps is surprising considering the similarities between the complexes.

### AACVD of mixtures of 3 & 4

The XRD patterns of all the compositions displayed cubic patterns as expected for PbE solids. Fig. 3(a) shows three patterns all showing a cubic pattern with shifts in all reflections across the patterns as the selenium content is increased. Inspection of the 422 reflection over increments of  $x_{\text{Se}} = 0.05$  is shown in Fig. 3(b). The gradual shift in the 422 reflection can be seen from that of pure PbS,  $x_{\text{Se}} = 0$ , to pure PbSe,  $x_{\text{Se}} = 0.5$ . The movement across the entire mole fraction range is shown in

Fig. 3(c). A linear relationship between the mole fraction of the precursors in the CVD flask and the position of the 422 reflection can be observed between  $x_{\text{Se}} = 0$  and 0.4. From  $x_{\text{Se}} = 0.5$  to 1 the 422 reflection matches with the position in the PbSe reference pattern (ICDD 00-006-0354) indicating that the bis[*N,N*-diethyl-*N'*-2-naphthoylthioureato]lead(II) is no longer being incorporated into the films. Linear regression of the region between  $x_{\text{Se}} = 0$  and 0.4 results in a minimum  $x_{\text{Se}}$  of 0.43 for pure PbSe.

Comparison of the film composition by ICP-AES with the lattice constant,  $a$ , allows for examination in relation to Vegard's law, Fig. 4. The films exhibited a linear change in the lattice parameter with decreased sulphur content. This matches with the predicted behaviour of  $\text{PbS}_x\text{Se}_{1-x}$  which is expected to show a subtle deviation from linear behaviour.<sup>27</sup>

Scanning electron micrographs show dramatic variations in the size and shape of the nanocrystals formed when altering the precursor mole fraction as shown in Fig. 5. Variation in the nanocrystal size could be a consequence of the difference in the initial breakdown temperature of the two complexes as shown in the TGA profiles, Fig. 2. The PbSe samples, *i.e.* where

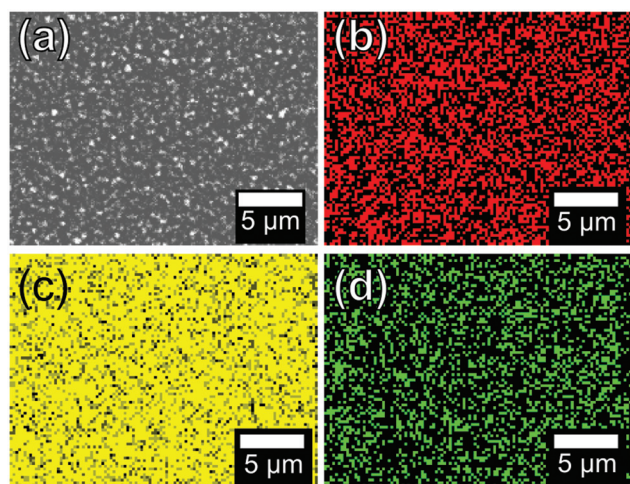


Fig. 4 (a) A plot showing the relationship between the mole fraction of the precursor used and the resulting composition of the film of  $\text{PbS}_x\text{Se}_{1-x}$ . (b) A Vegard plot for the  $\text{PbS}_x\text{Se}_{1-x}$  films between the mole fraction of the Se precursor,  $x_{\text{Se precursor}}$ , 0 to 0.6. Composition of the produced films was determined by ICP-AES analysis of Pb and Se. The dashed line represents ideal Vegardian behaviour between PbS and PbSe using  $a$  from ICDD PbSe 00-006-0354 and ICDD PbS 00-005-0592.



Fig. 5 Scanning electron micrographs of  $\text{PbS}_x\text{Se}_{1-x}$  films produced from  $x_{\text{Se precursor}} = 0, 0.1, 0.2, 0.3, 0.4, 0.5$  and 0.6 represented by (a) to (f) respectively.





**Fig. 6** An SEM image for the alloyed films produced using  $x_{\text{Se (precursor)}} = 0.3$  (a) and the corresponding EDX maps for Pb, S and Se (b), (c) and (d) respectively.

$x_{\text{Se (precursor)}}$  is 0.5 & 0.6 (e & f), show distinctly larger nanocrystals and less uniform films. EDX mapping was used to confirm that a uniform alloy was made, Fig. 6, with Pb, S and Se being found evenly spread across the film. Photographs of the films showed the typical dark brown colour when moving through the range of compositions of the  $\text{PbS}_x\text{Se}_{1-x}$  films, ESI Fig. 2.†

## Conclusions

AACVD of bis[*N,N*-diethyl-*N'*-2-naphthoylthioureato]lead(II) and bis[*N,N*-diethyl-*N'*-2-naphthoylselenoureato]lead(II) mixtures has successfully been used to make  $\text{PbS}_x\text{Se}_{1-x}$  films of controlled chalcogen compositions. The combination of precursors successfully makes alloyed nanocrystals and not two populations of nanocrystals of binary lead chalcogenide compositions. The precursors used performed as ideal single source precursors for AACVD due to the absence of additional undesired phases from the other elements present in the precursor. The relationship between the mole fraction of bis[*N,N*-diethyl-*N'*-2-naphthoylselenoureato]lead(II),  $x_{\text{Se}}$ , and the position of the 422 reflection is linear between  $x_{\text{Se}} = 0$  and 0.43.

## Conflicts of interest

There are no conflicts to declare.

## Acknowledgements

POB and PDM would like to acknowledge funding from the Engineering and Physical Sciences Research Council (EPSRC) grants # EP/K010298/1 and EP/K039547/1. TEE and POB would

like to thank the Nigerian Government for the PhD studentship that supported TEE.

## Notes and references

- 1 N. O. Boadi, M. A. Malik, P. O'Brien and J. A. M. Awudza, *Dalton Trans.*, 2012, **41**, 10497–10506.
- 2 N. L. Pickett and P. O'Brien, *Chem. Rec.*, 2001, **1**, 467–479.
- 3 M. A. Malik, M. Afzaal and P. O'Brien, *Chem. Rev.*, 2010, **110**, 4417–4446.
- 4 M. Afzaal, K. Ahmad and P. O'Brien, *J. Mater. Chem.*, 2012, **22**, 12731–12735.
- 5 M. Afzaal, K. Ellwood, N. L. Pickett, P. O'Brien, J. Raftery and J. Waters, *J. Mater. Chem.*, 2004, **14**, 1310–1315.
- 6 T. Trindade and P. O'Brien, *Chem. Vap. Deposition*, 1997, **3**, 75–77.
- 7 M. J. Moloto, N. Revaprasadu, G. A. Kolawole, P. O'Brien and M. A. Malik, *S. Afr. J. Sci.*, 2005, **101**, 463–465.
- 8 J. Akhtar, M. Akhtar, M. A. Malik, P. O'Brien and J. Raftery, *J. Am. Chem. Soc.*, 2012, **134**, 2485–2487.
- 9 J. Akhtar, M. A. Malik, S. K. Stubbs, P. O'Brien, M. Helliwell and D. J. Binks, *Eur. J. Inorg. Chem.*, 2011, **2011**, 2984–2990.
- 10 M. Akhtar, J. Akhtar, M. A. Malik, F. Tuna, M. Helliwell and P. O'Brien, *J. Mater. Chem.*, 2012, **22**, 14970–14975.
- 11 N. O. Boadi, P. D. McNaughton, M. Helliwell, M. A. Malik, J. A. M. Awudza and P. O'Brien, *Inorg. Chim. Acta*, 2016, **453**, 439–442.
- 12 J. S. Ritch, T. Chivers, K. Ahmad, M. Afzaal and P. O'Brien, *Inorg. Chem.*, 2010, **49**, 1198–1205.
- 13 A. C. Onicha, N. Petchsang, T. H. Kosel and M. Kuno, *ACS Nano*, 2012, **6**, 2833–2843.
- 14 T. Duan, W. Lou, X. Wang and Q. Xue, *Colloids Surf., A*, 2007, **310**, 86–93.
- 15 L. Bolundut, I. Haiduc, G. Kociok-Khön and K. C. Molloy, *Rev. Roum. Chim.*, 2010, **55**, 741–746.
- 16 N. Pradhan, B. Katz and S. Efrima, *J. Phys. Chem. B*, 2003, **107**, 13843–13854.
- 17 J. Akhtar, M. Afzaal, M. A. Vincent, N. A. Burton, I. H. Hillier and P. O'Brien, *Chem. Commun.*, 2011, **47**, 1991–1993.
- 18 J. M. Clark, G. Kociok-Kohn, N. J. Harnett, M. S. Hill, R. Hill, K. C. Molloy, H. Saponia, D. Stanton and A. Sudlow, *Dalton Trans.*, 2011, **40**, 6893–6900.
- 19 P. D. McNaughton, J. C. Bear, A. G. Mayes, I. P. Parkin and P. O'Brien, *R. Soc. Open Sci.*, 2017, **4**, 170383.
- 20 P. D. McNaughton, S. A. Saah, M. Akhtar, K. Abdulwahab, M. A. Malik, J. Raftery, J. A. M. Awudza and P. O'Brien, *Dalton Trans.*, 2016, **45**, 16345–16353.
- 21 E. A. Lewis, P. D. McNaughton, Z. Yin, Y. Chen, J. R. Brent, S. A. Saah, J. Raftery, J. A. M. Awudza, M. A. Malik, P. O'Brien and S. J. Haigh, *Chem. Mater.*, 2015, **27**, 2127–2136.



- 22 J. Akhtar, M. A. Malik, S. K. Stubbs, P. O'Brien, M. Helliwell and D. J. Binks, *Eur. J. Inorg. Chem.*, 2011, **2011**, 2984–2990.
- 23 S. A. Saah, P. D. McNaughten, M. A. Malik, J. A. M. Awudza, N. Revaprasadu and P. O'Brien, *J. Mater. Sci.*, 2018, **53**, 4283–4293.
- 24 I. B. Douglass, *J. Am. Chem. Soc.*, 1937, **59**, 740–742.
- 25 I. B. Douglass and F. B. Dains, *J. Am. Chem. Soc.*, 1934, **56**, 1408–1409.
- 26 G. M. Sheldrick, *Acta Crystallogr., Sect. A: Found. Crystallogr.*, 2008, **64**, 112–122.
- 27 Naeemullah, G. Murtaza, R. Khenata, N. Hassan, S. Naeem, M. N. Khalid and S. Bin Omran, *Comput. Mater. Sci.*, 2014, **83**, 496–503.

